Modelling Chloride Ingress into in-Service Cracked Reinforced Concrete Structures Exposed to De-icing Salt Environment and Climate Change

Abbas S. AL-Ameeri [a,b] M. Imran Rafiq [b], Ourania Tsioulou [b] and Oyuna Rybdylova [c]

[a] Engineering College, University of Babylon, Babylon, Iraq.
[b] School of Architecture , Technology and Engineering, University of Brighton, Brighton, UK.
[c] School of Computing, Engineering and Mathematics, University of Brighton, Brighton, UK.

ABSTRACT

The greenhouse gases (GHG), in terms of CO_2 emissions, have influenced the climate system by altering the planet's temperature and relative humidity (RH) patterns creating global warming. These changes in temperature and RH could be increased the penetration rate of chloride in existing concrete structures causing an acceleration of degradation processes that have the tendency to influence the serviceability and safety of these structures. There is a flurry of models to predict chloride penetration, however only very limited models aims to predict the chloride concentration profiles as a function of time, temperate and RH in cracked concrete members which is the characteristic of any existing concrete structures. The factors affecting chloride concentration and penetration in concrete are categorized as 'internal' (relating to the characteristic material properties such as porosity and crack width) and 'external' (relating to the environmental parameters, such as Temperature and RH). The fundamental aim of this research is to develop an integrated deterioration prediction model of chloride concentration and penetration in concrete structures considering the impacts of variations in the internal and external factors. The model is based on simultaneous solutions of diffusivity of chloride ions and it is validated using the data obtained from accelerated chloride penetration experiments. It is then used to investigate the chloride concentrations in existing concrete structures due to the impact of climate change scenarios based on the IPCC, 2014 and the UKCP'09 climate projections.

Keyword: Chloride penetration, numerical model, climate change, chloride concentration profiles, crack width

1. Introduction and background

The performance requirements of concrete structures are the design, construction and maintenance, which are affected by deterioration over time and impacts the safety, serviceability, and durability of these structures. The degradation rate in concrete structures depend not only on the quality of construction and material composition but is also impacted by the external environment conditions [1]. Therefore, the durability of concrete structures could be affected directly or indirectly by the climate change, in association with the change in

CO_2 concentration, temperature and RH. Climate change is defined as: " any change in climate over time, whether due to natural variability or as a result of human activity" [2]. The increase in CO_2 emissions plays a vital role in the climate system changes by affecting the global atmosphere [3]. At the same time, the global warming can be caused an increase in air, surface and seawater temperatures which in turn could cause glaciers to melt and sea level to rise. For example, the average temperature in central England has increased by 1ºC since the 1970s and is likely to rise more as a result of the influence of human activities on the environment [4].

IPCC (2007) and UKCP'09 (2010) propose climate projections (scenarios) for the 21st century and beyond. According to these scenarios, there is an increase in CO_2 concentrations and temperature and a drop in RH over this period. As an example, UKCP'09(2010) models (projections) forecast the increase in mean summer temperature in parts of southern England of up to 4.2°C by 2080. Also, relative humidity is expected to be reduced by around 9% in the same period. Whereas, in the Scottish islands, the expectation is that the temperature will increase by up to 2.5°C.

The climate-related deterioration of concrete structures is mostly caused by the infiltration of deleterious substances from the environment, such as CO_2 and chloride penetration, which cause corrosion of reinforcement in concrete structures [5, 6]. The temperature in concrete members due to environmental exposure is the main factor influencing the durability of concrete structures, carbonation, chloride penetration and the corrosion rate of steel bars in the concrete structures. The temperature response of the concrete illustrates obvious hysteresis features compared with the climate temperature variations due to the thermal properties of the concrete. Therefore, to predict the temperature response in concrete in a natural climate environment, Yuan and Jiang (2011) [7] proposed a model based on the behaviour of the concrete's thermal conduction. Climate-change induced acceleration of the corrosion process by accelerating the penetration of carbon dioxide (carbonation) [8] and chloride ions. This acceleration in the corrosion process by a few per cent may result in amplified maintenance costs annually [1].

Chloride ions are transported into concrete primarily from external sources such as de-icing salt, seawater and groundwater, and internal sources through contaminants (particularly found in some old structures) in concrete such as marine aggregates and chemical admixtures containing chloride ions)[9]. The transport of chloride within un-cracked concrete is a combination of the concentration gradient (diffusion), the pressure gradient (permeation) and capillary sorption) [9, 10].

Cracks in concrete structures are expected due to its low tensile strength. Cracks can be either non-structural or structural. Structural cracks often result from one, or a combination, of the following factors: insufficient reinforcement, low strength of concrete, excessive loading magnitude or frequency. While, the non-structural cracks may occur due to physical, chemical and thermal impacts such as drying shrinkage, carbonation shrinkage and thermal impact of freeze and thaw cycle) [11, 12]. There are different methods to monitoring the cracks propagation such as acoustic emission [13, 14].The cracks in concrete introduce an additional impact within the transport properties of concrete, namely the permeability of concrete, which is likely to significantly increase the transport of chloride ions inside concrete [15]. These results are not fully in agreement with the results obtained in [15, 16] due to natural formation of cracks in the sample (width, depth and tortuosity) or the method of assessing the diffusion coefficient of chloride.

The studies of durability assessment in literature, such as corrosion initiation, often exclude the effect of chloride penetration, carbonation and cracks, voids and defects in concrete, thereby their effectiveness in predicting the durability of concrete structures is reduced [16]. Therefore, it is important to investigate the influence of the de-icing salt environment, climate change and in-service cracks on the penetration of chloride and the degree

of corrosion. Moreover, chloride ions negatively affect the passive protective film (PPF) of steel reinforcement in concrete structures [17], which accelerates the corrosion of reinforced concrete structures [9, 18].

The factors affecting chloride concentration and penetration in concrete are categorized as 'internal' (relating to the characteristic material properties such as porosity and crack width) and 'external' (relating to the environmental parameters, such as Temperature and RH). The focus of this study is to propose an integrated model for chloride concentration in concrete structures (cracked and un-cracked concrete samples) under combined impacts of internal and external factors, for de-icing salt environment and climate change.

2. Experimental Programme

2.1 Materials and Mix Designs

In order to validate chloride penetration model and to quantify the influence of main parameters on chloride concentration and penetration depth, experimental tests were carried out. These tests were designed to accurately determine the concentration and depth of chloride under different environmental conditions of chloride concentration, such as different relative humidity and temperature conditions. For these purposes, the concrete samples were cast, cured, and exposed to accelerated chloride testing method in a CCT chamber at the University of Brighton laboratories. In this chamber, temperature and chloride concentration were automatically controlled. To achieve various properties of concrete, different water to cement ratios were used. Portland limestone cement (CEM II/A-LL 32,5R) with a specific gravity of 3.05 was used in this study. Natural sand was used as fine aggregate (particle size < 5mm), and the coarse aggregate used was crushed gravel with the size ranging from 5-14 mm. The mixture proportions (water, cement, sand and gravel) were designed according to the Research Establishment method (1988) [19] and the mixture proportions (water, cement, sand and gravel) and mechanical properties of these mixtures were listed in Table 1.

Table 1: Concrete mix designs used in this study

Mixture symbol	Content per unit volume of concrete (kg / m^3)					Mechanical properties	
	w/c	Cement	Water	Sand	Gravel	Comp. Strength MPa	Porosity %
M 0.4	0.4	513	205	653	980	53.2	10.1
M 0.5	0.5	410	205	711	1023	48.1	11.1
M 0.6	0.6	350	205	711	1041	39.7	12.5

2.2 Methodology

100*100*500 mm reinforced concrete prisms and 100 mm cubes were cast in two layers, demoulded and cured in a sink filled up with tap water for 28 days. The concrete prisms were stored in a lab environment condition (25 °C, 60% RH) for some time to dry and achieve a uniform moisture profile in the concrete surface. In this study, three different crack width ranges, (0, 0.05-0.15mm, 0.15-0.25mm and 0.25-0.35mm) and uncracked were applied to concrete prisms. The flexural method was used to induce the cracks, reinforced concrete prisms were used by fixing reinforcement in moulds with concrete cover 20 mm to control on the crack width in concrete prisms. The one face of the specimens was exposed to accelerated environment conditions through the cyclic chloride spraying, utilising a CCT chamber (see Figure1) and other faces were sealed (using multiple coats of water-based alkyl polysiloxane resin). The CCT chamber accelerates the chloride penetration into the concrete. The samples of each series were conditioned in the CCT chamber for 16 weeks; each 12 hours cycle consisted of 6 hours of chloride solution spray (5% concentration of NaCl). The tank of CCT chamber

was regularly topped up with a freshly prepared salt solution, followed by 6 hours of the dry environment both at a fixed temperature of (20°C, 30°C and 40 °C) respectively.

The conditioned samples were taken from the chloride chamber and split into two parts using a compression testing machine. The face of the sample was drilled closed to the crack locations to collect concrete powder samples at a seven various depth intervals using dry drilling equipment to establish total chloride concentration profiles by chloride titration method according to BS EN 12390- 11:2015 [20]. Three samples were tested for each case. The collected concrete powder was sieved using 150 micro-meter sieves to reduce the amount of coarse grains (resulted from the aggregate), then dried in an oven at 50°C for 24 hours, and then kept in sealed plastic bags till chloride titration testing to find the total chloride concentration profiles for all samples and mixtures.

The scenarios, chloride concentration, temperature, and relative humidity were selected to assess the impact of time and types of concrete for each environment condition factor on concentration and depth of chloride in these types of concrete. Chloride concentration (5% concentration of NaCl), relative humidity level ranged (75-100 %) and three temperature degrees (20°C, 30°C and 40 °C) have been separately used (see Figure 2), each scenario was ran for 16 weeks. The scenarios and series are shown in Table 2. For each type of mixture, and each crack width case and each series, twelve specimens of concrete were prepared. This provided a total of 108 prisms prepared and exposed to chloride resistance testing for this study.

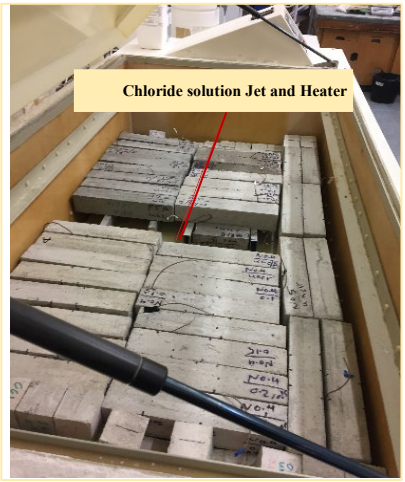

Figure 1: Chloride spraying chamber to accelerate chloride penetration

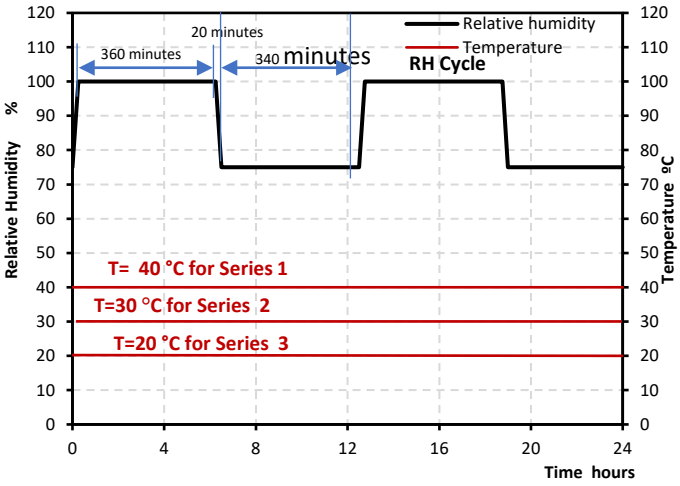

Figure 2: Cyclic wetting and drying cycles for chloride exposure

Table 2: Scenario of environment exposure condition of the experimental programmes

Scenarios	Series No.	Environmental exposure condition			Duration of exposure (weeks)
		CO_2 (%)	Temperature (°C)	Humidity (%)	
Scenario	1	Atmosphere , 400 ppm	40	As shown in Figure 2	16
	2		30		16
	3		20		16

3. Model development and verification

3.1 Mechanism for Chloride Penetration in Concrete

The transportation of chloride ions in aqueous solutions within concrete occur mainly through pore spaces in the cement paste matrix or micro-cracks [9, 21]. A variety of different physical and/or chemical mechanisms may govern the transport of chloride ions into the concrete. Chloride ingress in concrete depends on the flow of chloride ions and their local concentration, the environmental conditions (temperature and relative humidity), the pore water structure of concrete, the pore radius or width of micro-cracks and the degree of saturation of the pore system [22].

Considering the wide range of pore sizes and a varying moisture concentration in the concrete as a function of the climatic exposure conditions, the transportation of chloride ions into concrete in most cases is not due to one single mechanism. However, several mechanisms may act simultaneously. Chloride transportation into concrete can be a combination of the concentration gradient of chloride ions, the pressure gradient and capillary sorption making the flow of chloride through pores by combined transport methods such as diffusion, permeation and capillary sorption [9, 23].

3.2 Frame Work for Chloride Penetration Model

The two mechanisms for chloride transport in cementitious materials under usual conditions are considered in this model. (i) Diffusion, i.e., the transportation of chloride ions within the pore solution caused by their concentration gradient. (ii) Convection, i.e., the transportation of chloride ions together with the pore solution within the concrete caused by the moisture/humidity gradient) [10, 24]. These methods are a diffusive- convective–phenomenon. One-dimensional ingress of chloride ions into partially saturated concrete due to both diffusion and convection can be described using the following partial differential Equation [25]:

$$\frac{\partial C_{Cl}}{\partial t} = -\frac{\partial}{\partial x}\left[D_{eff}\frac{\partial C_{Cl}}{\partial x} + u_D C_{Cl}\right] + R_{Cl} \qquad (1)$$

where: C_{Cl} is the total concentration of chloride ions (kg of Cl^- per m^3 of concrete), D_{eff} is the effective chloride diffusion coefficient (m^2/s), u_D is the Darcy Law coefficient which describes the humidity diffusion or so-called velocity vector of ions due to the bulk movement of pore solution phase (m/s), R_{Cl}: bound chloride due to the reaction of chloride with cement compounds, and t denotes time (s).

The computational domain, the initial, and the boundary condition of Equation 1 are the following:

$$C_{Cl}(x,t) \qquad 0 \le x \le d \quad and \quad 0 \le t \le \infty \qquad (2)$$

$$C_{Cl}(x,0) = C_i \qquad \text{for} \quad t = 0 \qquad (3)$$

$$C_{Cl}(0,t) = C_s \qquad for \quad t > 0 \qquad (4)$$

$$\frac{d}{dx}C_{Cl}(L,t) = 0 \qquad zero - flux\ boundary \qquad (5)$$

where: C_s is surface chloride concentration; d is the total depth of sample and C_i is the initial value, which sometimes is assumed zero, and L is the depth of sample.

The flowchart for the development of model accounting for the chloride penetration of the concrete structure is illustrated in Figure 3.

3.3 Diffusion Coefficient of Chloride

The transportation of chloride ions is mainly affected by the density of concrete, ρ, the porosity of media ($\in$), tortuosity of pores (Ω) and degree of saturation of porous media (S) as shown in Equation 6 [21].

$$D_{eff} = \frac{\in S}{\Omega\, \rho} D_a \qquad (6)$$

where: D_a is the apparent chloride diffusion coefficient.

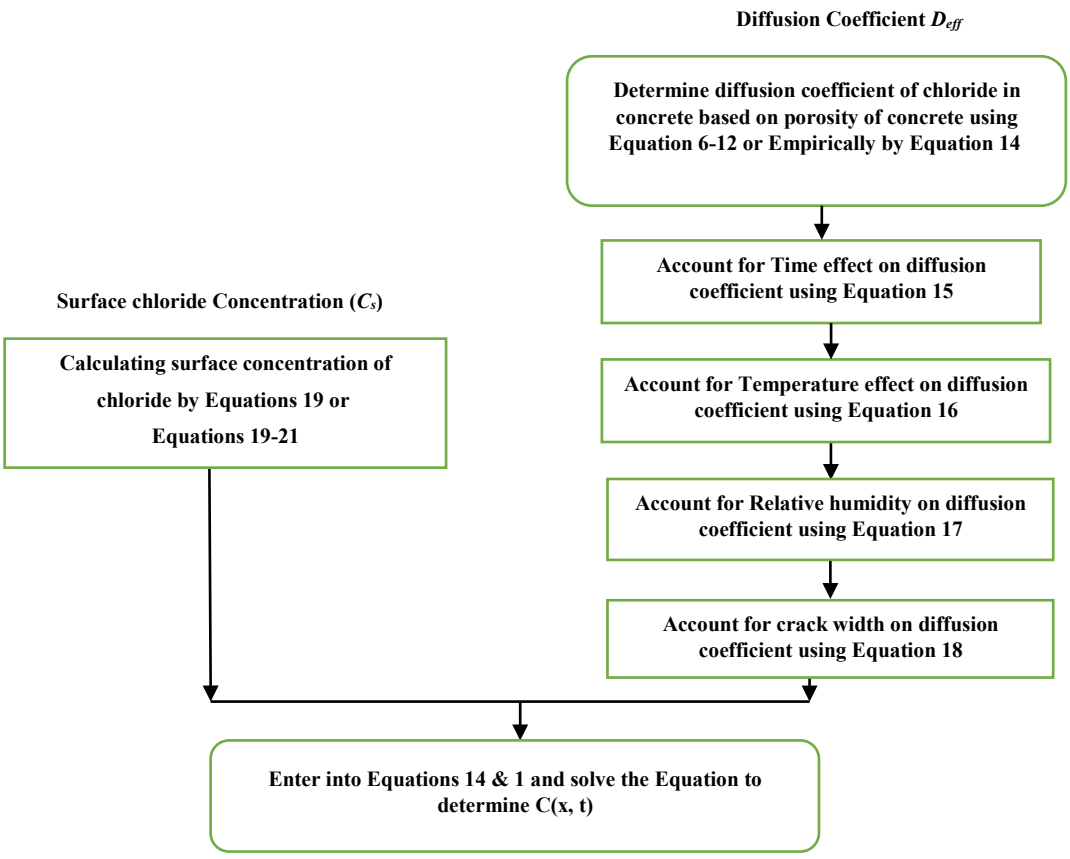

Figure 3: Flowchart for the determination of chloride profile

Only capillary and gel pores, which can act as transport paths for chloride ions, or locations for chemical reactions, are considered. The porosity in cement paste is the sum of the volume of the capillary pores and the gel pores to a total volume of cement paste, while in concrete the porosity,$\in$ is the sum of the porosity of the cementitious paste pores, aggregate pores and voids in an intermediate transition zone, ITZ zones between cement paste and aggregate.

Diffusion paths of chloride ions in concrete are constrained because micro-structure of concrete in terms of pore structure is often tortuous compared with diffusion paths ions in free water and directions of paths of diffusion are not parallel to the concentration gradient. Tortuosity (Ω) is presented to account for this complex micro pore structure of concrete. Tortuosity is a reduction factor in terms of chloride permeation rate due to the complexity of

the micro-pore structure of concrete mass as shown in Figure 4 and the tortuosity is a function of porosity in cement paste as shown in Equation 8 [21].

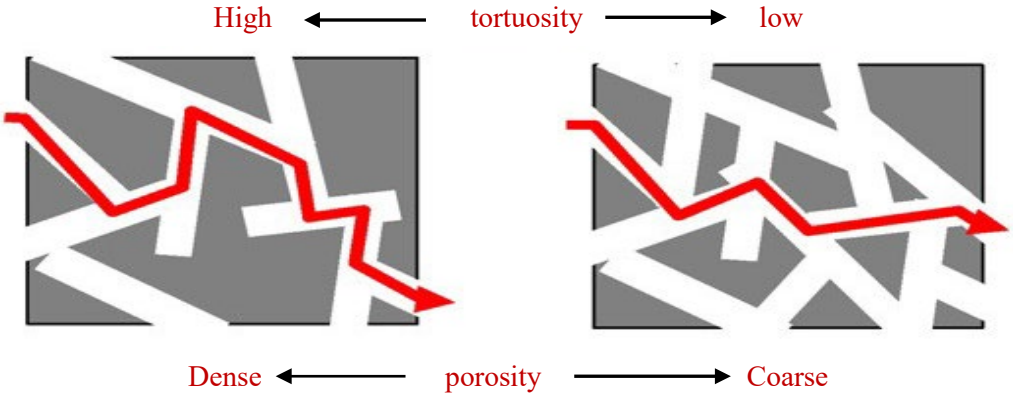

Figure 4:Schematic of micro-pore structure of concrete and tortuosity (Ω) [21]

where: $\emptyset_{paste}$ is the porosity of capillary and gel pores in cement paste (m^3/m^3).

The influence of tortuosity on the chloride concentration profile for two cases can be Ω = 1.9 for porosity equal to 0.3 and Ω = 3.0 for porosity equal to 0.2 %. The value of the degree of saturation of porous media (S) changes according to the moisture in the pore structures. The value of (S) can lie between 0 to 1. It is difficult to account for measure the tortuosity and degree of saturation because it is necessary to measure the path direction of pores and the volume of water. In this study, Ω and S will be taken as 3 and 1 respectively.

There are two approaches to an estimate of the diffusion coefficient of chloride: Scientific modelling and empirical modelling.

(i): Scientific modelling for D_a:

This type of modelling is based on a scientific activity or basic knowledge about the phenomenon under study and seeks [26]. In this study, modelling of D_a is based on the different chemical and physical processes that are involved during the ingress of chloride. The transport and mass balance equation considering the interaction between the ions in the pore solution and the cementitious matrix is also considered. Basically, the diffusion coefficient of chloride in pore solution (free space) (D_{Cl}) is expressed according to Nernest-Einstein's theorem [21], when the concentration of chloride ions is around 3% NaCl (by mass) by:

$$D_{Cl} = RT\frac{\lambda_{ion}}{Z_{Cl}^2F^2} \quad (8)$$

where: R is the gas constant (8.314 J/ mol K), T: temperature (K), Z_{Cl} is the electric charge of the chloride ion (=−1C), F is Faraday's constant (9.65×10^4 C/mol), λ_{ion} is ion conductivity ($S.m^2/mol$).

Concerning the molar conductivity of an ion, λ_{ion}, may be affected by temperature dependency, the influence of temperature in λ_{ion} is considered according to the Arrhenius's Law [27] as shown:

$$\lambda_{ion} = \lambda_{(25)}exp\left[-\frac{E_a}{R}\left(\frac{1}{T}-\frac{1}{298}\right)\right] \quad (9)$$

where: $\lambda_{(25)}$ is ion conductivity at 25°C, $\lambda_{25}=7.63\times10^{-3}$ ($S.m^2/mol$), E_a is the activation energy for free pore fluid (17.6×10^3 (J/mol)). The D_{Cl} at 25 °C is 2.0310^{-9} m^2/sec. The activity of

chloride ion in penetration or diffusion coefficient can be increased by 12% if the temperature is increased to 30 °C.

Essentially, the size and connectivity of the pore structures are considered the main path of diffusion of fluid in concrete and this system of pores mainly depends on the water/cementitious materials (w/cm) ratio [17,28]. When the porosity and w/c ratio are lower, the pore system and path of transportation of chloride ions may be tight, which gives a lower transport rate of fluid and a lower active diffusivity. In order to find the diffusion coefficient of chloride in concrete, the term ($D_{a,ref}$) needs to consider the pore volume percentage in cement paste (V_v), based on the quantity of water remaining and not used in the hydration process as estimated by Papadikas and Tsimas (2002) [29]. The fraction of aggregate in concrete factor (f_{agg}) was assumed by Shi *et al*. (2014) [28].

$$D_{a,ref} = D_{Cl}\, V_v\, f_{agg} \tag{10}$$

$$V_V = \left(\frac{\frac{w-0.267(C+P)}{\rho_W}}{\frac{C}{\rho_C}+\frac{P}{\rho_P}+\frac{W}{\rho_W}} \right)^3 \tag{11}$$

$$f_{agg} = \frac{1-V_a}{1+V_a} \tag{12}$$

where: C is the cement content (kg), w is the water content (kg), ρ_C is the absolute density of cement (3150 kg/m^3), ρ_W is the density of water (1000 kg/m^3), ρ_P is the absolute density of supplementary cementing materials(1800-2800 kg/m^3), V_a is aggregate weight to concrete weight ratio and P is the amount of supplementary cementing materials(kg).

(ii): Empirical modelling of the coefficient of chloride, D_a:

This type of modelling generally utilize experimental data to predict chloride ingress in concrete. The time dependency of D_a and some of the other parameters have been considered to propose the empirical models of D_a. It was found that the most critical factor influencing apparent diffusion of concrete is the porosity of concrete and the w/c ratio has a significant impact on the porosity of the concrete. Therefore, the correlation between apparent diffusion coefficient D_a and effective porosity or w/cm can be used to model the depth of chloride penetration due to exposure to wet-dry cycles of chloride solution. The experimental results of this study shows the exposure temperature considerably affected the penetrability of chloride in concrete samples. Finally, D_a can be considered as a function of a concrete type, w/cm ratio and exposure condition e.g. temperature RH and the duration of exposure and age of concrete.

From the experimental data obtained through this study on normal concrete (without supplementary cementitious materials), the influence of w/c and temperature (T) on apparent diffusion coefficient, D_a (as shown in Equation 13 and Figure 5) has been calculated by linear regression analysis using the statistical programme, Statistics. The main data from Series 1, 2 and 3 were used in this analysis to find the w/cm and temperature influence. The correlation coefficient (R) was 0.9384 and all correlations were statistically significant at the P= 0.0017 level.

$$D_a = \left(1.3889 + 18.3333\, \frac{w}{c} + 0.3\, T\right) 10^{-12} \tag{13}$$

where: The apparent diffusion coefficient, D_a in m^2/s at 15 weeks of exposure duration and the temperature, T is in (°C).

In addition to the period of duration exposure and the age of the concrete, D_a is thought to be a function of concrete type, w/cm ratio and exposure condition e.g. temperature and relative humidity. Val and Trapper (2008); Vu and Stewart (2000) [25, 30] considered the effect of temperature, T, pore relative humidity on D_a, but they were not considered the influence of crack and properties of concrete on the D_a. On the other hand, Sheo-Feng *et al.* (2011) [31] reported the crack width, W_c on diffusion chloride coefficient based on an artificial crack without taking into consideration the type of concrete. This study focuses on the effects of global climate change, temperature, relative humidity and cracks width as well as the properties of concrete (different types of concrete). Therefore, the simulation of D_a, these parameters, T, RH, W_c and properties of concrete will be taken into consideration (Equation 14) to predict chloride concentration with a depth of concrete and time to determine the initiation of corrosion time due to chloride penetration.

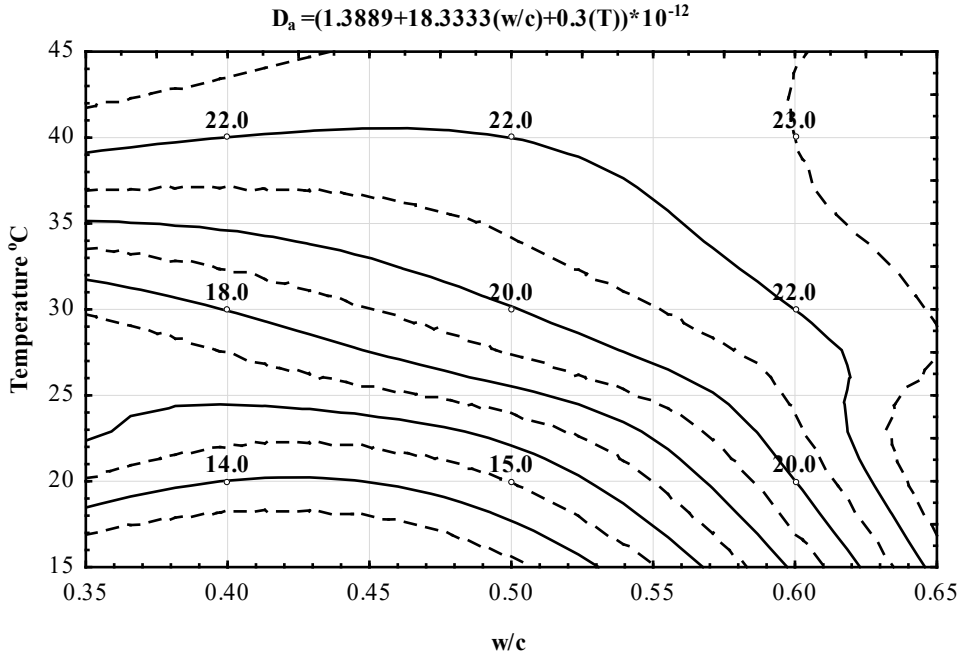

Figure 5: Effect of w/cm ratio and temperature on apparent diffusion coefficient (D_a = *10^{-12} m^2/sec)

$$D_a = D_{a,ref} f_{C1}(t) f_{C2}(T) f_{C3}(RH)\, f_{C4}(W_c) \qquad (14)$$

where: $D_{a,ref}$ is the value of D_a at reference condition (i.e. at the reference temperature, time and relative humidity) and it can be obtained by either Equation 9 or 13, $f_{c1}(t), f_{c2}(T), f_{c3}(RH)$ *and* $f_{c4}(W_c)$ are functions of time, temperature, relative humidity and crack width, respectively. Analytical explanation of these factions will be given in the following section.

a. Time-Dependent Component of D_a

Bamforth *et al.* (1997) [30] reported the D_a decreased rapidly in the first five years, beyond that it may be a constant value. Takewaka and Mastumoto (1988) [33] proposed the dependency of this coefficient $D_a(t)$ on the exposure period t , using empirical formula which

designates the reduction of diffusion coefficient with time according to the materials (e.g. mixture proportions) and the environment (e.g. temperature and humidity) by.

$$f_{c1}(t) = \left\{\frac{t_{ex}}{t}\right\}^{m}, t>t_{ex}\ ,\ 0 \le m \le 1 \qquad (15)$$

where: t_{ex} is initial exposure time, t is a specific time and m is the ageing factor (diffusivity reduction factor), depending on the development of strength of the concrete, w/cm ratio and type of cementitious materials used in mortar /concrete such as cement, silica fume, fly ash and GGBS and environmental conditions [34]. In experimental results, the ageing factor values were 0.21-0.65 according to w/cm ratio. CEB-FIP (2010); ACI Committee 365(2018); Wang *et al*. (2016) [35, 36, 37] reported the ageing factor is likely to be between 0.2 and 0.8.

b. Temperature Dependent of D_a

The impact of temperature `is based on the Arrhenius Equation. The diffusivity of chloride ions in concrete is one of the chemical reactions. The diffusivity of Cl^- can be broken down into two sequences, the Cl^- spreads in concrete and dissolves into the pore water coating the pore walls and some of the amount of chloride may react with dissolved hydrated products of cement which form Friedel's salt. Val and Trapper (2008); Thomas *et al*. (2012) [25, 38] have proposed Equation 16 to simulate the temperature dependence of the diffusion coefficient of chloride in concrete.

$$f_{c2}(T) = exp[\frac{U_c}{R}(\frac{1}{T_{ref}} - \frac{1}{T})] \qquad (16)$$

where: U_C is the diffusion activation energy. The activation energy for chloride diffusing in concrete has been experimentally determined by Page *et al*. (1981) [39], depending on its water-cementitious materials ratio (w/c) and it is 41.8±4.0 (kJ/mol) for w/c = 0.4, 44.6±4.3 (kJ/mol) for w/c = 0.5, and 32.0±2.4 (kJ/mol) for w/c = 0.6. R is the gas constant (8.314 J/mole. K), T_{ref} is a reference temperature (298 K) and T is the temperature of interest (K).

c. Relative Humidity Dependent Component of D_a

Relative humidity or moisture content is one important factor influencing the chloride penetration in concrete. In other words, moisture content controls the availability of chloride and oxygen at the concrete-steel interface surface [40]. Val and Trapper (2008) [25] have proposed the function of relative humidity related to chloride penetration in terms of diffusion of chloride coefficient, as given in Equation 17.

$$f_{c3}(h) = \left[1 + \frac{(1-h)^4}{(1-h_c)^4}\right]^{-1} \qquad (17)$$

where: $f_{c3}(h)$ is a function of relative humidity, h is the humidity percentage, h_c is the critical humidity level at which the diffusion coefficient drops halfway between its maximum and minimum value (hc=0.75) [25].

d. Crack Dependent Component of D_a

The presence of cracks and permeable pores in concrete has a significant impact on diffusion and permeation of chloride ions in concrete [31]. The type and width of the crack influence the penetration of chloride in concrete. Results of previous studies have shown that the crack opening significantly influences the ability of chloride ions to diffuse along a crack. On the other hand, no chloride diffusion occurs in cracks with an opening of critical value

(threshold value) or less [41]. At crack openings greater than the threshold value, chloride diffusion along the crack path depends on mortar age [42]. The chloride ions mainly penetrate the sides of the crack-like external layer of the sample.

From the experimental data obtained through this research (on normal concrete without the use of supplementary cementitious material), the influence of crack width (W_c) on the apparent diffusion coefficient, D_a (as shown in Equation 18 and Figure 6) has been calculated by non-linear regression analysis using the statistical programme, Statistics. The main data from experimental works were used in this analysis to find the crack factor influence, $f_{c4(Wc)}$. The correlation coefficient (R) was 0.956 and all correlations were statistically significant at the P= 0.000 level (see Figure 7).

$$f_{c4(W_c)} = 0.934{W_c}^2 + 0.974W_c + 1 \qquad (18)$$

where: $f_{c4(Wc)}$ is Proportion of diffusion coefficient in the cracked sample ($D_{a(cracked)}$) to diffusion coefficient in the un-cracked sample ($D_{a(un\text{-}cracked)}$); W_c is the crack width in mm.

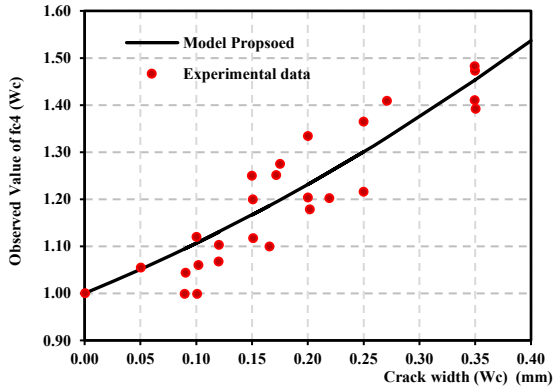

Figure 6: Effect of crack width on Chloride diffusion due to cracked factor ($f_{c4(Wc)}$)

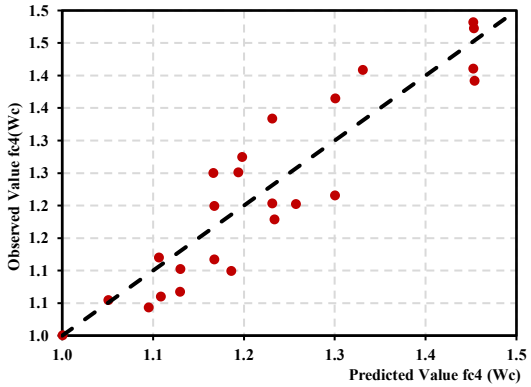

Figure 7: Observed and predicted values of the model proposed of cracked factor ($f_{c4(Wc)}$)

3.4 The Surface Concentration of Chloride

The surface concentration of chloride ions on the first layer of the sample can be obtained according to environmental conditions. In addition to the time and age of exposure, the surface concentration of chloride, C_s is thought to be a function of concrete properties, w/cm ratio [43], exposure environment e.g. marine and de-icing state (ACI Committee 365: 2018; Song *et al*., 2008) [36,44] and exposure condition e.g. temperature and relative humidity.

Firstly, for concrete structures exposed to the de-icing environment, Kassir and Ghosn (2002) [45] proposed a surface chloride concentration model based on field investigations by testing 15 bridge's decks exposed to deicing salt in the snow belt region for 15 years.

$$C_s = C_o(1 - e^{-\alpha t}) \qquad (19)$$

where: C_o is the maximum value of chloride (5.343 kg/m^3), α is the age factor and equal to 0.25 (year $^{-1}$), and t is the time measured in years.

A ramp-type surface chloride concentration was applied by Phurkhao and Kassir (2005) [46] for surface chloride on bridge decks which is mainly derived from de-icing salt and t_o as shown in Equations 21 and 22.

$$C_s(t) = \frac{C_o}{t_o}\, t \qquad 0 \le t \le t_o \qquad (20)$$

$$C_s(t) = C_o \qquad t \ge t_o \qquad (21)$$

3.5 Numerical Analysis of Chloride Penetration in Concrete Structures

The finite element methods have become a commonly used method to solve a group of applications in engineering fields. The finite element method, FEM is based on the separation of structures into a finite elements number linked by nodes [47]. In the present study, a non-linear finite element technique (NLFET) was used to determine chloride ions concentration profile by finding the diffusivity of chloride ions in concrete using the FEM package Multiphysics. In this case, Multiphysics was used to simulate the chloride concentration profile depth in concrete and Transport of Diluted Species in Porous Media Method (tds). The transportation of diluted species interface supports the simulation of chemical species transport by convection and diffusion in one dimensional (1D), two dimensions (2D), and three dimensions (3D) as well as for axisymmetric models: (i) Mass Balance Equation (ii) Convective Term Formulation and (iii) Solving a Diffusion Equation.

3.5.1 Frame Work of Numerical Analysis of Species Diffusion

The numerical results of the diffusivity of chloride ions (Cl^-) in different concrete specimens were plotted. All the samples were modelled with the FE package of Multiphysics. Where the diffusivity of Cl^- has been modelled. Numerical analysis of diffusivity is based on properties of concrete samples; some properties were obtained from experimental work such as density, porosity, and compressive strength. While, the other parameters were computed from the proposed model in the first section such as the chloride diffusion coefficient in section 3, whilst the modulus of elasticity, Poisson's ratio was based on the proposed equations by AL-Ameeri *et al*. (2013) and AL-Ameeri and AL-Rawi (2009) [48, 49] respectively. Thermal conductivity, *Tc* is given from relationships of ACI 122R (2002) [50]. The steps using numerical analysis is shown in Figure 9. Some of the samples were un-cracked and the others were cracked.

3.5.2 Model Geometry and Meshing using Programme

The geometry of the full specimen was defined by a three-dimensional full specimen (100*100*500 mm). The mesh settings determine the resolution of the finite element mesh used to discretize the model. The finite element technique is the method to divide the model into small elements of geometrically simple shapes. This was achieved by defining boundary conditions.

Figure 8 demonstrates the simple schematic of the mesh model geometry of concrete samples (with and without a crack) which were modelled as collected together to simulate this model. The concrete was modelled with a 3-node free triangle element available in the programme's element library. This element type has concentrated integration stiffness [51].

This element can be also used for nonlinear analysis counting that of integration. The maximum and minimum element size of the mesh, and the curvature factor was 1.3 mm, 0.004 mm and 0.6 respectively.

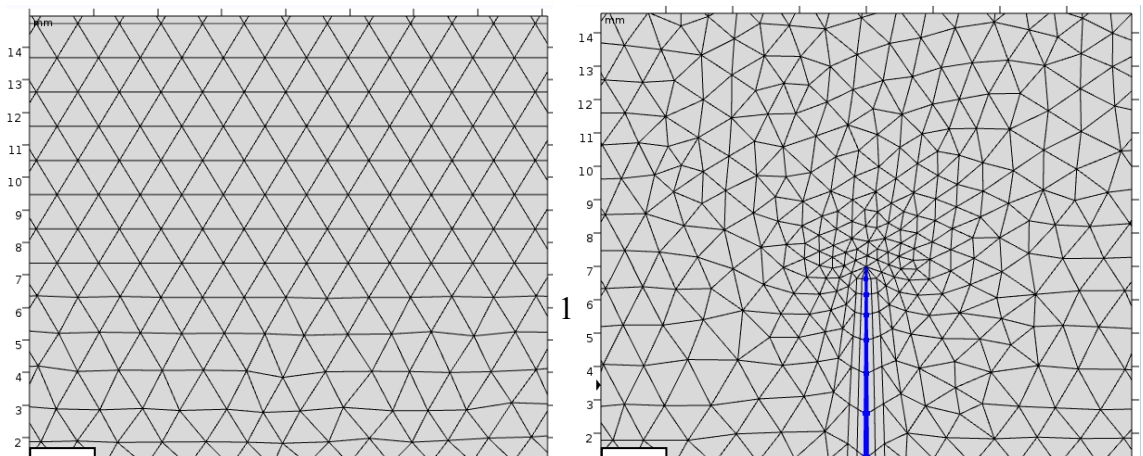

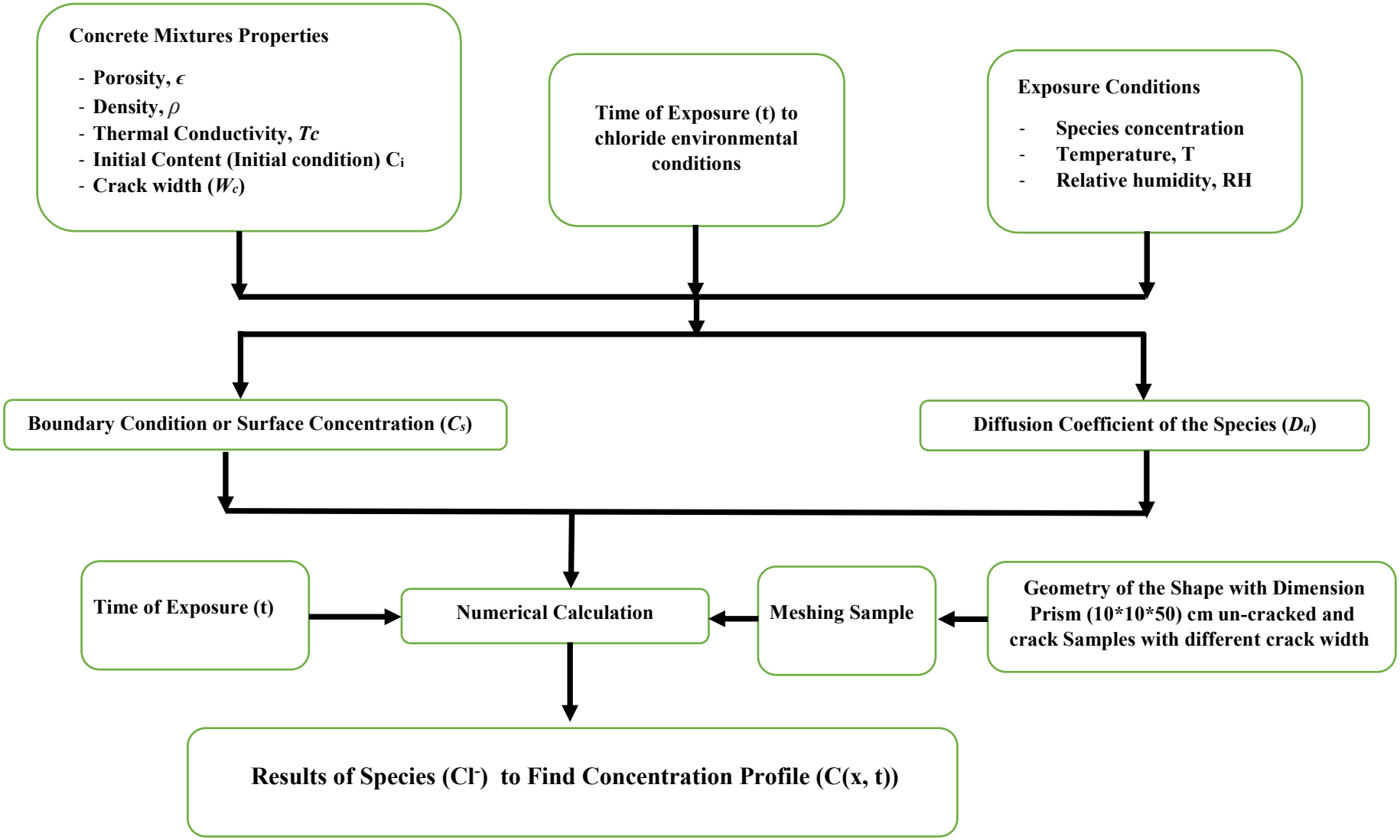

Figure 9: Flowchart of numerical analysis using the FEA programme

4. Verification of Numerical Analysis of Chloride Concentration in Concrete Samples

The verification of the chloride transport model was done by comparing two types of experimental results for two cases, un-cracked and cracked.

In the experimental programme, 108 concrete prisms (10*10*500 cm) were tested. These were un-cracked and cracked respectively. For the un-cracked and cracked specimens, different w/c ratios were tested, while for the cracked ones, different crack width and depth were examined. These specimens were exposed to chloride spraying with 5% NaCl on one surface for about 115 days to simulate the penetration of chloride in a one-dimensional flow, as presented in Figure 10.

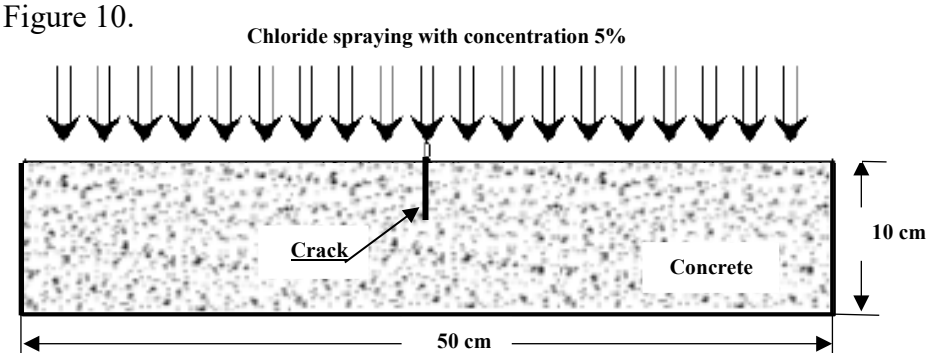

Figure 10: Schematic of sample exposed to chloride spraying condition

The profile of total chloride content was measured by the titration technique and the results of the cases are tested.

In this study, a finite element programme was used to solve Equation 1, which governs the time-dependent mass transfer of chloride and convection flow. The programme is validated by comparing its results with available experimental data collected in the experimental programme.

The use of FEA is based on the computed properties of concrete and the mixture. For any arbitrary initial state (in this case, initial chloride content was 0.26-0.5 % by mass of cement according to the mixture proportion) and boundary conditions or membrane (in this case, surface chloride concentration), the vapour pressure in pores (u_D), relative humidity (RH), and moisture distribution or degree of saturation (S) are mathematically simulated according to a moisture transport model (convection) that considers both vapor and liquid phases of mass transport (diffusion).

The moisture distribution, RH, and micro-pore structure characteristics, in turn, control the Cl^- diffusion and rate of various chemical reactions under arbitrary environmental conditions (e.g temperature) [21]. In this section of the study, the chloride transportation in uncracked and cracked concrete will be simulated as shown in Figure 10. The diffusion chloride coefficients (D_a) for the sample are computed according to Equations 6-18 and presented in Tables 3.

While, surface chloride concentrations (C_s) are used for experimental data. In this study, un-cracked and three crack width levels were simulated. The width and depth of crack were measured and calculated respectively to find the relationship between them as crack width 0.05-0.15mm, 0.15-0.25mm and 0.25-0.35 mm with crack depth 20, 30 and 35 mm respectively. To simplify the analysis, a numerical analysis was used by (FEM) to compute the chloride concentrations profile, $C\ (x,\ t)$ as shown in Figure 8. Where, simulation figures of chloride concentration profile show the influence of the crack in an increase of penetration and concentration of chloride with an increase in the crack width and depth as shown in Figure 11.

Table 3: $D_{a,\,ref}$ value with fraction aggregate, pore volume ratio, temperature, relative humidity, and crack width

Sample	V_a	f_{agg}	V_v	$D_{a,}$ at 40 °C m^2/sec *10^{-12}			
				Un-cracked	**0.05-0.15 mm**	**0.15-0.25 mm**	**0.25-0.35 mm**
M 0.4	0.695	0.180	0.185	21	22	26	29
M 0.5	0.738	0.151	0.320	19.6	23.6	26.5	29.3
M 0.6	0.759	0.137	0.353	23.3	26.6	30	33.4

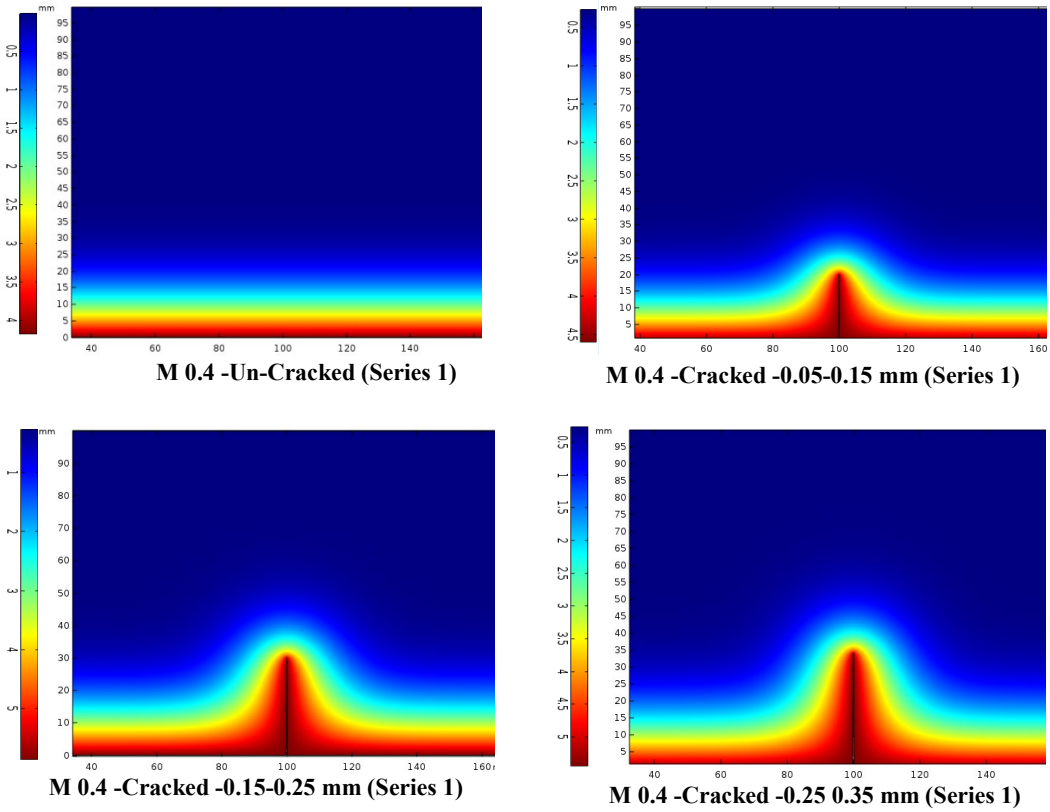

Figure 11: Chloride concentration distribution in the samples with and without a crack due to exposure to chloride environment at 40 °C for 115 days

The computational results of chloride concentration which are gotten from the partial differential equation showed in Equation 1 compared with experimental results for Series 1 (at temperature 40 °C) (cracked and Uncracked) are presented in Figure 11 according to Ning and Li (2015) [52]. A qualitative difference in trend is seen in the square of this correlation coefficient, R^2 between the model predicted and the experimental results as shown in Figure 12 and in Table 4. The analytical results from using a model based on diffusion-convection illustrated the shape of the distribution of chloride concentration obtained from the analysis and experimental data were well-matched. Where, in the analytical results, the surface concentration was relatively high, with a trend of a sharp reduction in chloride concentration with depth. On the other hand, the experimental results using the titration method in the test showed the actual measured value of chloride concentration at the first point of depth was a

curve that is convex downwards. This kind of anomaly between both results has been reported in the past research as well [21].

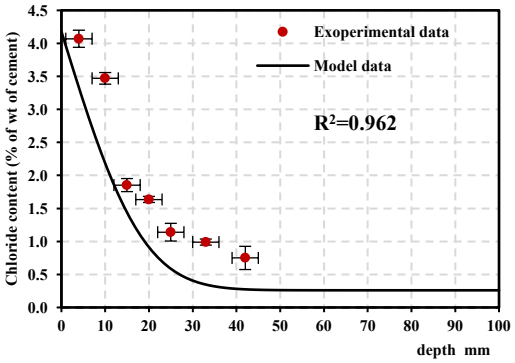

a: M 0.4 Un-Cracked (Series 1)

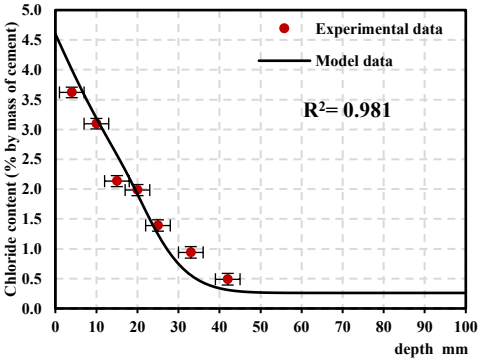

b:M 0.4 Cracked -0.05-0.15 mm (Series 1)

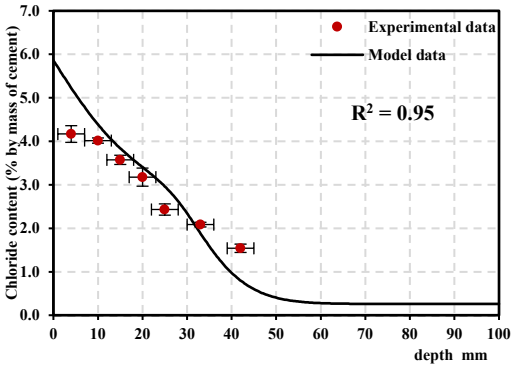

c:M 0.4 Cracked -0.15-0.25 mm (Series 1)

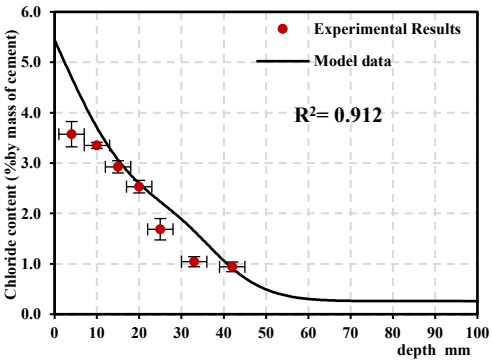

d:M 0.4 Cracked -0.25-0.35 mm (Series 1)

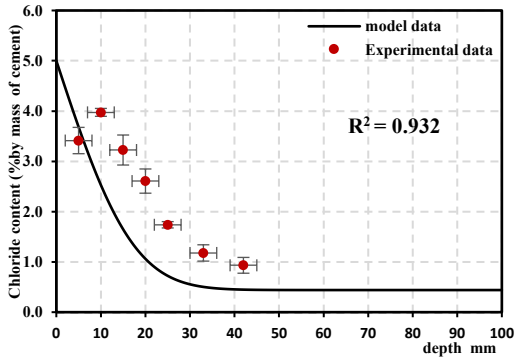

e:M 0.5 Un-Cracked (Series 1)

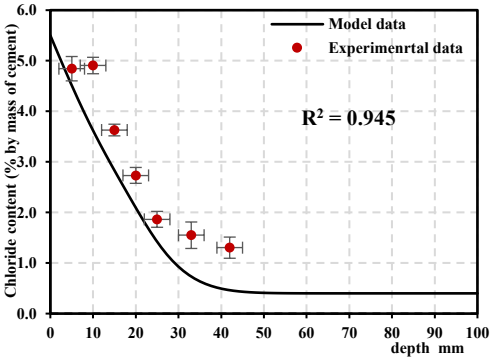

f:M 0.5 Cracked -0.05-0.15 mm (Series 1)

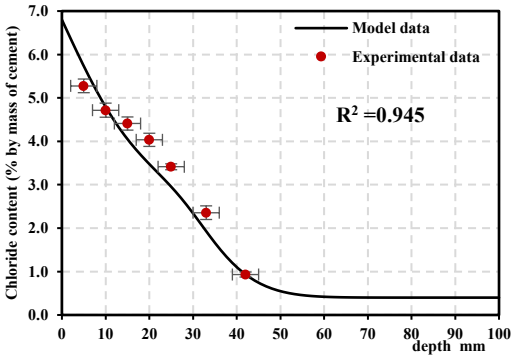

g:M 0.5 Cracked -0.15-0.25 mm (Series 1)

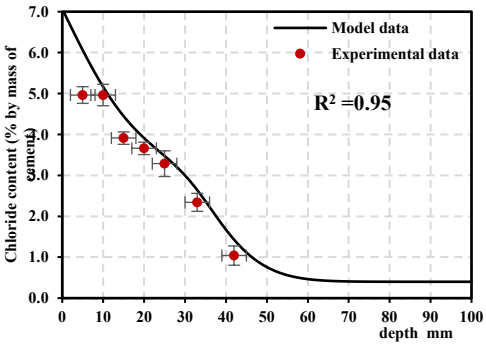

h:M 0.5 Cracked -0.25 0.35 mm (Series 1)

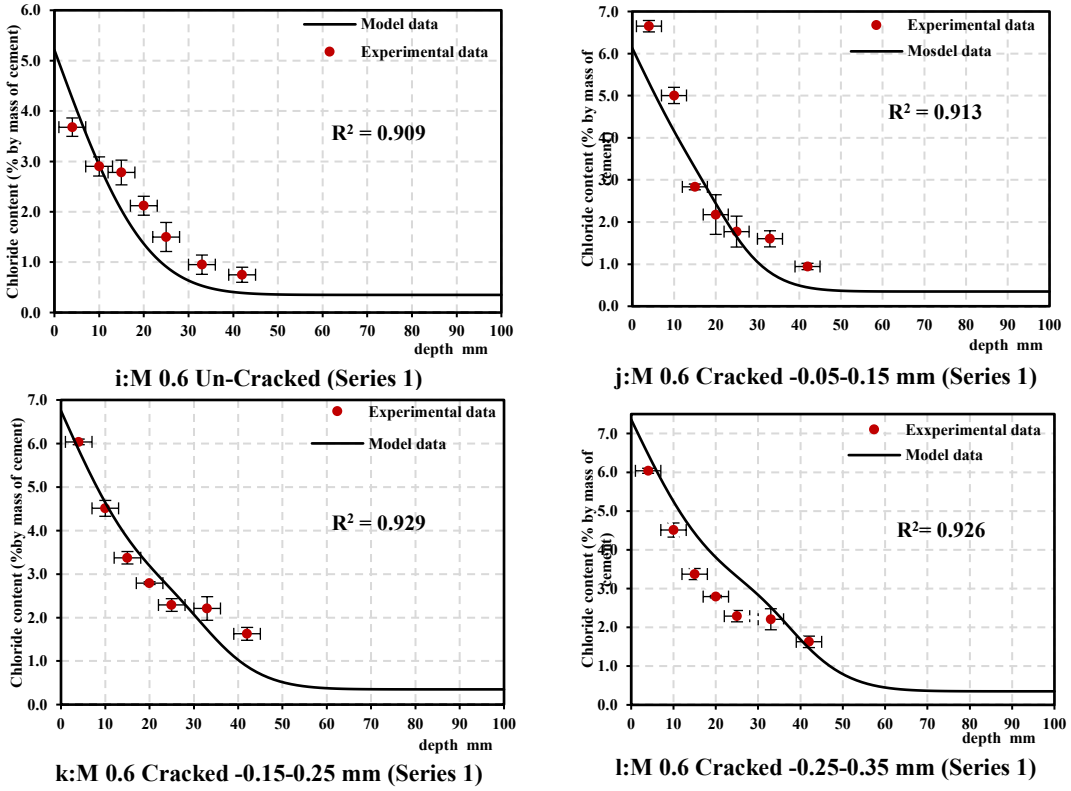

Figure 12: Chloride concentration, numerical vs experimental results for Series 1(40 ^{o}C)

Table 4: Correlation coefficient, R^2 of model predicted chloride concentration and the experimental results for Series 2(30 ^{o} C) and Series 3(20 ^{o} C)

Sample	Un-cracked		0.05-0.15 mm		0.15-0.25 mm		0.25-0.35 mm	
	Series 2	Series 3	Series 2	Series 3	Series 2	Series 3	Series 2	Series 3
M 0.4	0.947	0.915	0.986	0.984	0.881	0.984	0.973	0.846
M 0.5	0.983	0.931	0.978	0.948	0.989	0.941	0.985	0.850
M 0.6	0.989	0.96	0.977	0.976	0.965	0.974	0.964	0961

It can be seen from Figure 12 and Table 4, the analytical data of model matched well with the experimental results in about 33 of the 36 figures (the R^2 values of the most of these graphs were more than 0.90). The fit is less favourable in these cases; however, the trends are still correct even here. Overall, this model (in Equations 1 and 4) can be used to forecast the chloride concentration profile in concrete with different scenarios of chloride exposure (e.g. marine and de-icing salts).

5. Prediction of Chloride Concentration in Concrete Structure due to Climate Change

The surface chloride concentration of the environment is the main driving force for chloride penetration in concrete structures. The model selects the rate of chloride build-up and the maximum surface concentration based on the type of exposure (and structure) and the geographic location or the severity of exposure of concrete structures to environment chlorides

(ACI 365- 2018) [36]. There are two main categories of exposure environments, can be classified into two levels of chloride concentration, de-icing and sea water salt, due to the concentration of chloride solution and number of repeated cycle exposed to concrete structures,

In this study, the first category of chloride exposure condition relates to the structures exposed to de-icing salts e.g. bridge decks and parking structures, will be considered. While, the second category of chloride exposure condition relates to the structures exposed to seawater salts e.g. platform in marine structures, will be studied in another study (Part 2). The exposure of the concrete sample to an accelerated environment condition is quite different from the exposure of the sample to de-icing salt. Where, in the accelerated method, the concentration of chloride solution and the number of repeated exposure cycles is much higher than the exposure of the concrete to deicing salt. Therefore, the surface chloride content can be higher because of C_s or the boundary condition is approximately linear in increase with the increase of the concentration of solution up to 15% [53]. In the case of de-icing salt, the main two scenarios of surface chloride concentration in concrete structures with time and can be used to forecast the C_s in concrete structures are listed as follows:

(i): Life-365 (2018) [36] assumes that initially, the C_s increases linearly with increasing time of exposure but remains almost constant after a period of time. The model determines the maximum surface chloride concentration reach the maximum C_s and the time taken to reach that maximum, depending on the type of structure (e.g. bridge deck), its geographic location and exposure based on field data. For example, the urban bridge assumes a maximum C_s between 0.68-0.85 (wt. % mass of concrete) depending on the usage of de-icing salt and the wash-off that happens on bridges exposed to rain and the rate of build-up varies by geographical location from 0.015 – 0.08 (% /year).

(ii) Phurkhao and Kassir (2005) [46] proposed a ramp-type surface chloride concentration applied for surface chloride of bridge decks as shown in Equations 20-21.

In this case, de-icing salt exposure, the hypothetical sample of the concrete structure in London city (case study) will be used to predict the chloride concentration profile due to this exposure environment condition (temperature, relative humidity, and climate change scenario). According to the proposed methodology of chloride concentration as shown in Figure 8, the calculation and assumption will be used as follows:

1- Concrete properties
- w/c ratio = 0.5, density =2400 kg/m^3, porosity = 0.12%.
- V_a =0.738, V_v = 0.32 and the fraction of aggregate factor, f_{agg}= 0.151.
- Initial content of chloride, C_i = 0.

2- Exposure condition
- Chloride spraying amount = 1 kg/m^2.
- Temperature as shown in Figure 13-a.
- Relative humidity as shown in Figure 13 -b.
- Climate change in Temperature will reach 4.2 ºC RH decrease by about 9% in 2080 (UKCP'09, 2010) [4].

3- Time of exposure: (25 and 50 years)

4- Boundary condition or surface concentration, C_s will use two approaches:
- Use the limitation of Life 365-2018 for urban structures where the C_s increases linearly between 0-8 years by 0 - 0.68 % by mass of concrete and is constant beyond 8 years at 0.68 % by mass of concrete.
- Use the limitation of Phurkhao and Kassir (2005) [46] for structures the C_s increases linearly between 0-5 year for 0 – 0.223 % by mass of concrete and be constant beyond 5 years at 0.223 % by mass of concrete.

5- The diffusion coefficient of chloride, D_a: It is computed and calibrated by age, and used crack width factor by Equations 7 to 19 (first assumption) and accounted temperature and relative humidity impact according to climate change with UKCP'09(2010) [4] models (scenarios) by same Equations (second assumption).
6- The shape of sample: deck slab which is 250 mm thick, one uncracked and another cracked with crack width 0.15 mm and depth 20 mm.

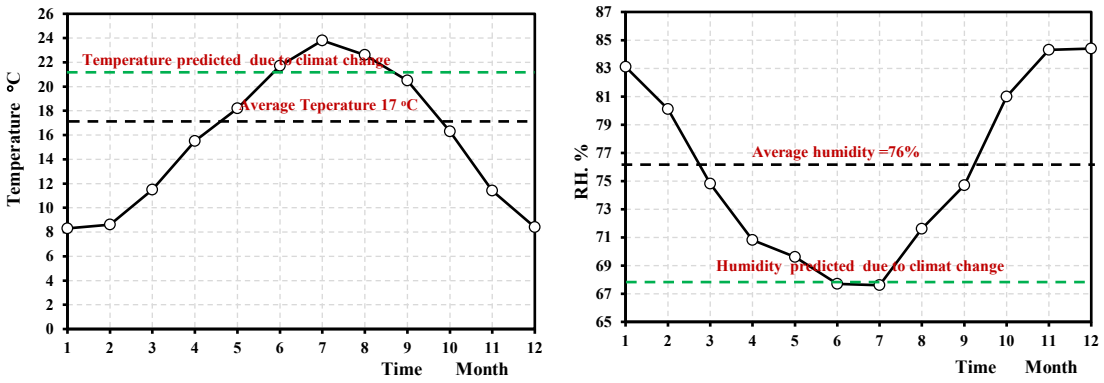

Figure 13: The annual maximum temperature and relative humidity of London (average of period 2004-2014) (Met Office- UK and UKCP'09, 2010)

According to the assumptions in example, the properties and type of exposure condition, the diffusion coefficient, D_a, and the effect of the time, temperature, humidity, and cracked factors are presented in Table 5. The C_s is derived based on two assumed approaches, Life 365:2018 and Phurkhao and Kassir (2005) [36, 46]. The Life 365: 2018 assumes the maximum C_s =0.68 (% by mass of concrete) at 7.5 years. Whereas, Phurkhao and Kassir (2005) [46] proposed the maximum C_s is 0.223 (% by mass of concrete) at 5 years. Both assumptions determine the C_s as being a constant beyond the maximum time. The C_s values for all cases are listed in Table 5.

Chloride profiles after 25 and 50 years of exposure for two cases (cracked with cracked width 0.15 mm and un-cracked) without the impact of climate change (in temperature and relative humidity) are shown in Figures 14 to 17. On the other hand, temperature and humidity factor at 25 and 50 years old due to climate change were considered in the chloride concentration profile and these factors affecting the diffusion coefficient were 1.1 and 1.25 respectively.

Figures 14-17 presents the predicted results for the chloride concentration profile in the concrete bridge deck exposed to the de-icing salts environmental conditions under the influence of climate change (change in temperature) according to UKCP'09(2010) [4] scenarios for two approaches and cases (cracked with cracked width 0.15 mm and Un-cracked).

Based on the above results, the chloride concentration for both exposure ages of simulation (25 and 50 years) increases by increasing the temperature and decreasing relative humidity due to climate change as the UKCP'09(2010) scenarios. The percentage increase of chloride concentration at depth 50 mm (minimum requirement of concrete cover) according to BS 8100: 1997 and BS 8500-1: 2015 [54, 55] is 4.6 % and 5.8% for exposure age, 25 and 50 years respectively (uncracked concrete bridge deck) for two approaches for C_s concentration. Whereas, the percentage for the cracked concrete deck (width 0.15 mm and depth 20 mm) for both approaches is 3.5% and 3.8% for exposure age, 25 and 50 years respectively.

1 Table 5: The Time, temperature, relative humidity and crack width dependent of D_a

Sample	D_a and at age and Temperature $m^2/sec *10^{-12}$, % (mass of concrete)							
	25 years old Without the effect of T and RH		25 years With the effect of T and RH		50 years old Without the effect of T and RH		50 years With the effect of T and RH	
	D_a	C_s	D_a	C_s	D_a	C_s	D_a	C_s
w/cm = 0.5 – un-cracked for (Life 365: 2018)	14	0.68	15.3	0.68	14	0.68	17.5	0.68
w/cm= 0.5 – un-cracked for Phurkhao and Kassir (2005)	14	0.22	15.3	0.22	14	0.22	17.5	0.22
w/cm= 0.5 –cracked 0.15mm mm for (Life 365: 2018)	17	0.68	18.6	0.68	17	0.68	21.3	0.68
w/cm= 0.5 –cracked 0.15mm for Phurkhao and Kassir (2005)	17	0.22	18.6	0.22	17	0.22	21.3	0.22

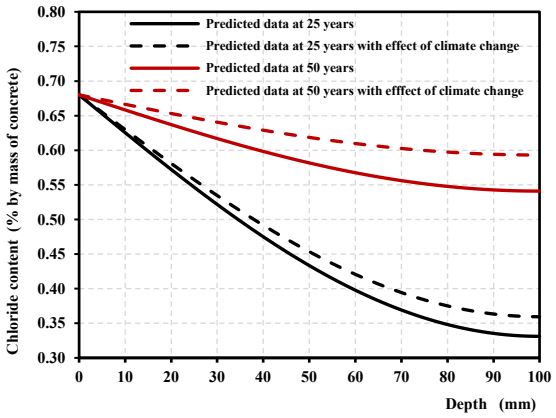

Figure 14: Model prediction of chloride concentration at un-cracked bridge deck in the city of London due to de-icing salt according to Life -365: 2018

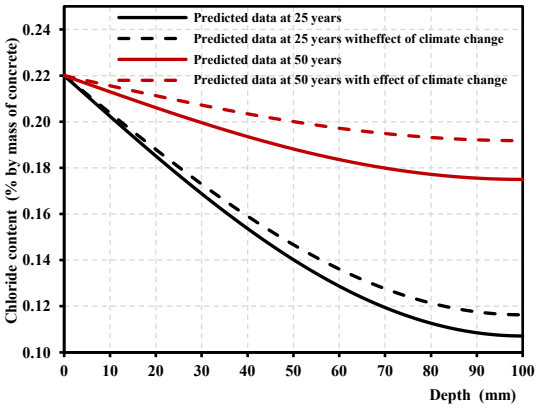

Figure 15: Model prediction of chloride concentration at un-cracked bridge deck in the city of London due to de-icing salt according to assumption Phurkhao and Kassir (2005)

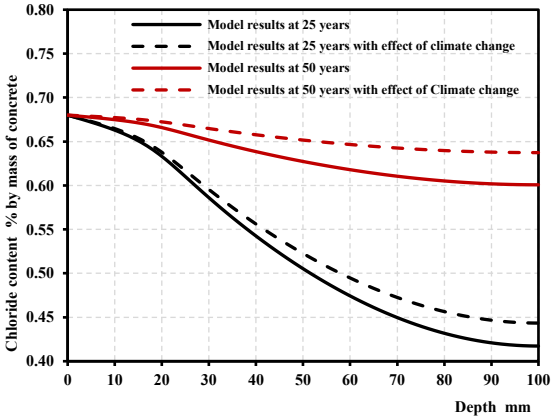

Figure 16: Model prediction of chloride concentration at cracked bridge deck (width 0.15 mm depth 20 mm) in the city of London due to de-icing salt according to Life 365: 2018

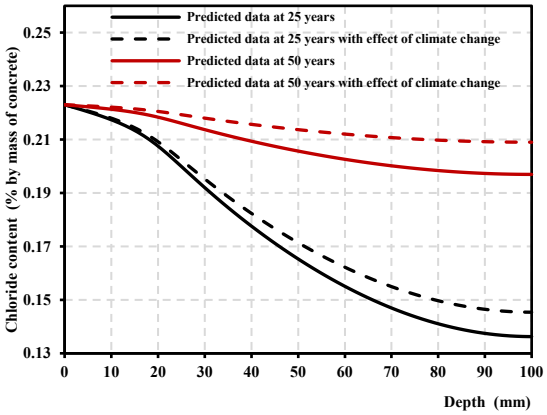

Figure 17: Model prediction of chloride concentration at cracked bridge deck (width 0.15 mm depth 20 mm) in the city of London due to de-icing salt according to assumption Phurkhao and Kassir (2005)

The results of the simulation for different surface chloride concentration and status of concrete (with and without a crack) as shown in Figures 14-17 illustrated the concentration of chloride content are affected significantly by a change in temperature and humidity due to climate change for both durations of exposure and status of the concrete surface, cracked and uncracked. These changes in chloride concentrations due to climate change (in temperature and humidity) have significant impact on diffusion coefficient of chloride, Da, because the Da has vital role on increase of chloride penetration and chloride penetration with depth into concrete .

In both cases, of cracked and un-cracked bridge deck concrete, the trend of predicted depths of chloride penetration by both approaches are relatively close in layers of concrete less than 20 mm deep. Beyond that depth, the influence of a change in temperature and humidity on chloride concentration increases with increasing depth of concrete for the two durations of exposure, 25 and 50 years. The percentage increase of chloride concentration at 50 years was higher than the percentage at 25 years due to an increase in chloride diffusion and an increase in temperature with the duration of exposure [25,38].

6. Conclusion

The modelling and simulation of the impact of climate change parameters on the durability of concrete structures, and in particular, on the chloride penetration is presented in this study. The modelling of chloride penetration has been developed and proposed to consider the 'internal' factors, such as the w/c ratio, porosity, tortuosity of voids in concrete (Ω) and the fraction of aggregate in concrete, and 'external' factors such as CO_2 concentration, temperature, RH. The modelling has been validated by extensive experimental results. Climate change and atmospheric temperature of UKCP'09(2010) scenarios were considered to predict rate of chloride penetrations within concrete.

1- A model has been developed for the prediction of the chloride profile (concentration with the depth of concrete) based on mechanisms of chloride transport methods in cementitious materials, the diffusion, and the convection or advective in concrete exposed to a salt solution under de-icing conditions.

2- In the modelling of chloride concentration, the effect of in-service cracks and external affected factors such as temperature and relative humidity was considered in deriving the diffusion chloride coefficient, D_a.

3- The modelling of chloride profile was based on Fick's Second Law of Diffusion and was solved numerically to establish the concentration of chloride within concrete depth and the time $C_{Cl}(x, t)$. The numerical model has been validated by experimental results from this study using two scenarios of both uncracked and cracked concrete samples. The results of the model proposed were generally a good fit and well-matched with the distribution of chloride concentration profiles obtained from concrete exposed to chloride conditions in these studies. Therefore, this modelling can be used to predict chloride concentration with the depths in the control condition and in future climate change scenarios. Two approaches of prediction of surface concentration C_s were used in environmental conditions, de-icing to investigate the impact of climate change on of chloride concentration profile in the long term of 50 years.

5- The influence of climate change (increase in temperature, and reduction of the relative humidity) has a significant impact on the chloride concentration profile as follows:

- For the de-icing environment condition (hypothetical sample of the concrete structure London city), the percentage increase in chloride concentration at a depth of 50 mm (minimum requirement of concrete cover) was 5.8 % and 3.8% for uncracked and cracked concrete decks respectively at an exposure age of 50 years for two approaches of C_s concentration.

- The impact of the crack on chloride concentration was observable for both environment conditions (de-icing and marine), duration of exposure and in both cases (the control case and the case including a climate change effect). The cracked concrete provide quickest route to speed up the chloride penetration and increases the chloride concentration into the un-cracked concrete surrounding the cracks.
- Climate change is observed to increase the progression of chloride concentration within concrete and induce corrosion in concrete structures at faster rate. The chloride concentration in deeper depths will be much higher in the long term and harsher exposure conditions such as the worst-case scenario of UKCP'09(2010).

References

[1] Wang, X., Stewart, M. and M. N. Nguyen (2012). "Climate change adaptation for corrosion control of concrete infrastructure." Structural Safety 35: 29-39.

[2] Bernstein, L., P. Bosch, O. Canziani, Z. Chen, R. Christ, O. Davidson, W. Hare, S. Huq, D. Karoly and V. Kattsov (2008). Climate change 2007: Synthesis report: An assessment of the intergovernmental panel on climate change, IPCC-2007.

[3] Pachauri, R. and L. Meyer (2014). "Climate change 2014: Synthesis report. fifth assessment report of the intergovernmental panel on climate change". Tech. Rep.

[4] UKCP'09,(2010). " UK Climate Projections science report: Climate change projections". [Online] available at: http://ukclimateprojections.defra.gov.uk.pdf.

[5] Tuutti, K. (1982). "Corrosion of steel in concrete". Stockholm, Swedish Cement and Concrete Research Institute.

[6] Chen, D. and S. Mahadevan (2008). "Chloride-induced reinforcement corrosion and concrete cracking simulation". Cement and Concrete Composites 30(3): 227-238.

[7] Yuan, Y. and J. Jiang (2011). "Prediction of temperature response in concrete in a natural climate environment". Construction and Building Materials 25(8): 3159-3167.

[8] AL-Ameeri, A., Rafiq, I., Tsioulou, O. and O. Rybdylova. Impact of Climate Change on the Carbonation in Concrete due to Carbon Dioxide Ingress: Experimental Investigation and Modelling. Journal of Building Engineering 44(2021)102594.

[9] Dyer, A. (2014). "Concrete durability". New York. Taylor& Francis Group, LLC.

[10] Basheer, L., J. Kropp and D. J. Cleland (2001). "Assessment of the durability of concrete from its permeation properties: a review ". Construction and building materials 15(2-3), 93-103.

[11] American Concrete Institute, ACI Committee 224. R, 01. Control of Cracking in Concrete Structures. (2001) Farmington Hills, Mich.: ACI.

[12] Concrete Society. Non-structural cracks in concrete, TR **22** (2010) Concrete Society.

[13] Ming, P., Lu, J., Liu, M., Cai, X., & Chen, X. (2021). Quantitative statistical analysis of the crack propagation and fracture process of self-compacting rubber concrete based on acoustic emission. Structural Control and Health Monitoring, 28(7), e2743.

[14] Li, X., Chen, X., Jivkov, A. P., & Hu, J. (2021). Investigation of tensile fracture of rubberized self-compacting concrete by acoustic emission and digital image correlation. Structural Control and Health Monitoring, e2744.

[15] Sheo-Feng, Z., Chun-Hua, L. and Rong-Gui, L. (2011). "Experimental determination of chloride penetration in cracked concrete beams". International conference on advanced in engineering, proceeding **24** ,380-384.

[16] Kwon S., Na U., Park S.and S.Jung (2009) "Service life prediction of concrete wharves with early-aged crack: a Probabilistic approach for chloride diffusion". Struct. Saf. J, **31**, 75–83.

[17] Neville, A. M. (2011). "Properties of Concrete ". 5th edition. London, Pearson Education Limited.

[18] Pacheco, J. and R. Polder (2010)"Corrosion initiation and propagation in cracked concrete – a literature review". Proceedings of the 4th International RILEM Ph.D. Workshop, Madrid, Spain.
[19] Teychenné, D.C, E Franklin, R.E. and H. C. Erntroy (1988), "Design of normal concrete mixes. Second edition". Building Research Establishment. Garston, Watford.
[20] European Committee for Standardization, BS EN 12390, Part 11(2015)." Testing hardened concrete: Determination of the chloride resistance of concrete, unidirectional diffusion". British Standard Institution.
[21] Ishida, T., T. Kishi and K. Maekawa (2014). " Multi-scale modeling of structural concrete ". Crc Press.
[22] Kropp, J. and H. Hilsdorf (2005). "Performance criteria for concrete durability". CRC Press.
[23] Morcous, G. and Z. Lounis (2005). "Prediction of onset of corrosion in concrete bridge decks using neural networks and case-based reasoning". Computer-Aided Civil and Infrastructure Engineering 20(2): 108-117.
[24] Martın-Pérez, B., S. Pantazopoulou and M. Thomas (2001). "Numerical solution of mass transport equations in concrete structures". Computers & Structures 79(13): 1251-1264.
[25] Val, D. V. and P. A. Trapper (2008). "Probabilistic evaluation of initiation time of chloride-induced corrosion". Reliability Engineering & System Safety 93(3): 364-372.
[26] Mason, R. L., R. F. Gunst and J. L. Hess (2003). "Statistical design and analysis of experiments: with applications to engineering and science ". John Wiley & Sons.
[27] Yokozeki, K., K. Watanabe, D. Hayashi, N. Sakata and N. Otsuki (2003). "Modeling of ion diffusion coefficients in concrete considering with hydration and temperature effects". Doboku Gakkai Ronbunshu 2003(725): 131-142.
[28] Shi, X., N. Xie, K. Fortune and J. Gong (2012). "Durability of steel reinforced concrete in chloride environments: An overview". Construction and Building Materials 30: 125-138.
[29] Papadakiss, V.G., S.Tsimas, (2002). “Supplementary cementing materials in concrete Part I: efficiency and design". Cement and concrete research 32(2002): 1525-1532.
[30] Vu, K. A. T. and M. G. Stewart (2000). "Structural reliability of concrete bridges including improved chloride-induced corrosion models". Structural safety 22(4): 313-333.
[31] Shao-feng, Z., L. Chun-hua and L. Rong-gui (2011). "Experimental determination of chloride penetration in cracked concrete beams". Procedia Engineering 24: 380-384.
[32] Bamforth, P., W. F. Price and M. Emerson (1997). "International Review of Chloride Ingress Into Structural Concrete". A Trl Report (Trl 359), Thomas Telford.
[33] Takewaka, K. and S. Mastumoto (1988). "Quality and cover thickness of concrete based on the estimation of chloride penetration in marine environments". Special Publication 109: 381-400.
[34] Broomfield, J. P. (2007). "Corrosion of steel in concrete: understanding, investigation and repair ". Taylor &Francis.
[35] International Federation for Structural Concrete, CEB-FIP (2013). "Model Code for Concrete Structures 2010". Wilhelm Ernst & Sohn, Verlag für Architektur und technische Wissenschaften GmbH & Co. KG, Rotherstraße 21, 10245 Berlin, Germany.
[36] American Concrete Institute, (2018). ACI Committee 365 Part 5. "Service-life prediction: state of the art report". Manual of concrete practice. Farmington Hills, Mich.ACI.
[37] Wang, J., P. M. Basheer, S. V. Nanukuttan, A. E. Long and Y. Bai (2016). "Influence of service loading and the resulting micro-cracks on chloride resistance of concrete". Construction and Building Materials 108: 56-66.

[38] Thomas, M., R. Hooton, A. Scott, et al. (2012). "The effect of supplementary cementitious materials on chloride binding in hardened cement paste". Cement and Concrete Research 42(1), 1-7.
[39] Page, C., N. Short and A. El Tarras (1981). "Diffusion of chloride ions in hardened cement pastes". Cement and concrete research 11(3): 395-406.
[40] Markeset, G. and R. Myrdal (2008). "Modelling of reinforcement corrosion in concrete-State of the art". COIN Project report no7, SINTEF Building and Infrastructure: 1891-1978.
[41] Ismail, M., A. Toumi, R. Francois and R. Gagné (2004). "Effect of crack opening on the local diffusion of chloride in inert materials". Cement and Concrete Research 34(4): 711-716.
[42] Ismail, M., A. Toumi, R. François, et al. (2008). "Effect of crack opening on the local diffusion of chloride in cracked mortar samples ". Cement and concrete research 38(8-9), 1106-1111.
[43] Chalee, W., C. Jaturapitakkul and P. Chindaprasirt (2009). "Predicting the chloride penetration of fly ash concrete in seawater". Marine structures 22(3): 341-353.
[44] Song, H.-W., C.-H. Lee and K. Y. Ann (2008). "Factors influencing chloride transport in concrete structures exposed to marine environments". Cement and Concrete Composites 30(2): 113-121.
[45] Kassir, M. K. and M. Ghosn (2002). "Chloride-induced corrosion of reinforced concrete bridge decks". Cement and Concrete Research 32(1): 139-143.
[46] Phurkhao, P. and M. Kassir (2005). "Note on chloride-induced corrosion of reinforced concrete bridge decks". Journal of engineering mechanics 131(1): 97-99.
[47] Cook, R. D. (2007). "Concepts and applications of finite element analysis". John Wiley & Sons.
[48] Al-Ameeri, A., K. AL-Hussain and M. Essa (2013). "Predicting a Mathematical Models of Some Mechanical Properties of Concrete from Non-Destructive Testing." Civil and Environmental Research 3: 78-97.
[49] AL-Ameeri, A. , R. AL-Rawi (2009). " A Study on Properties of Iraqi Steel slag as a Fine Aggregate in Concrete ". Journal of Building Technology, Saudi Arabia 13/2009.
[50] American Code Institute, ACI Committee 122 R. (2002). "Guide to thermal properties of concrete and masonry systems".
[51] Ngo, D. and A. Scordelis (1967). "Finite element analysis of reinforced concrete beams". Journal Proceedings, 64(3): 152-163.
[52] Ning, C. and B. Li (2015). "Probabilistic approach for estimating plastic hinge length of reinforced concrete columns". Journal of Structural Engineering 142(3), 04015164.
[53] Singhal, D., R. Agrawal and B. Nautiyal (1992). "Chloride resistance of SFRC. Fiber reinforced cement and concrete". Proceeding of the fourth international symposium held by RILEM, July 20th -23rd 1992, University of Sheffield.
[54] British Committee for Standardization, BS 8100 (1997). "Code of practice for design and construction". British Standards Institution.
[55] British Committee for Standardization, BS 8500-1 (2015). "Method of specifying and guidance for the specifier ". British Standards Institution.